

quicR: An R Library for Streamlined Data Handling of Real-Time Quaking Induced Conversion Assays

Gage R. Rowden^{a,b,c,*}, Peter A. Larsen^{a,b,c}

^aDepartment of Veterinary and Biomedical Sciences, University of Minnesota, USA.

^bMinnesota Center for Prion Research and Outreach, University of Minnesota, USA.

^cPriogen Corp., USA.

Abstract

Real-time quaking induced conversion (RT-QulC) has become a valuable diagnostic tool for protein misfolding disorders such as Creutzfeldt-Jakob disease and Parkinson's disease. Given that the technology is relatively new, academic and industry standards for quality filtering data and high throughput analysis of results have yet to be fully established. The open source R library, **quicR**, was developed to provide a standardized approach to RT-QulC data analysis. **quicR** provides functions, which can be easily integrated into existing R workflows, for data curation, analysis, and visualization.

Keywords: [R-package](#), [Chronic Wasting Disease](#), [RT-QulC](#), [Creutzfeldt-Jakob Disease](#), [Nano-QulC](#), [Micro-QulC](#), [RT-QulC](#), [prion diagnostics](#), [Creutzfeldt-Jakob](#), [Chronic Wasting Disease](#), [Parkinson's Disease](#), [seed amplification assay](#)

1 Metadata

1. Motivation and significance

Real-time quaking induced conversion (RT-QulC) is ~~a cutting-edge diagnostic assay that~~ [within the family of seed amplification assays \(SAAs\)](#), [similar to protein misfolding cyclic amplification \(PMCA\)](#), and has garnered significant attention for its ultra-sensitive detection of misfolded protein aggregates [1, 2]. The assay works by converting a recombinant protein substrate into an amyloid aggregate in the presence of a misfolded seed [1, 3, 4, 5, 6, 7, 8, 9, 10]. The assay's sensitivity and specificity make RT-QulC a promising tool for diagnosing diseases such as prion disorders and other protein misfolding pathologies [11, 12, 13, 14].

*Corresponding author.

¹E-mail address: rowde002@umn.edu

Nr.	Code metadata description	Metadata
C1	Current code version	V2.1.0
C2	Permanent link to code/repository used for this code version	https://github.com/gage1145/quicR/releases/tag/v2.1.0
C3	Permanent link to Reproducible Capsule	https://cran.r-project.org/web/packages/quicR
C4	Legal Code License	GPL-3
C5	Code versioning system used	Git
C6	Software code languages, tools, and services used	R
C7	Compilation requirements, operating environments & dependencies	R (>=4.1.0)
C8	If available Link to developer documentation/manual	https://cran.r-project.org/web/packages/quicR/quicR.pdf
C9	Support email for questions	rowde002@umn.edu

However, the relatively recent development and novelty of the assay have left a gap in widely accepted academic and industry standards for data analysis and interpretation [15].

To address this gap, we introduce **quicR**, an open-source library, developed in R [16], dedicated to the cleaning, analysis, and visualization of RT-QulC data. By consolidating key metrics and providing robust analytical tools, **quicR** aims to standardize the analysis pipeline and foster reproducibility within the field of quaking induced assays including related assays such as Nano-QulC [17] and Micro-QulC [18]. **quicR** is designed with both researchers and diagnosticians in mind, providing a user-friendly interface that integrates seamlessly with existing R workflows.

While universal diagnostic criteria for RT-QulC have yet to be established, certain analytical metrics have emerged as valuable tools for interpreting assay results and kinetics. These include:

1. Time-to-threshold (TtT): The time required for the fluorescence signal to exceed a predefined threshold ([also known as lag time](#)) [5].
2. Rate of amyloid formation (RAF): A measure of the kinetics of aggregate growth, which provides insight into the relative quantity of misfolded seed [19].
3. Maxpoint ratio (MPR): A ratio-based metric measuring peak normalized fluorescence intensities [15].
4. Maximum slope (MS): The steepest rate of fluorescence increase, reflecting the most rapid phase of aggregation [20].

Together, these metrics enable researchers to characterize the kinetics of RT-QulC reactions comprehensively, enhancing the rigor and reliability of diagnostic decisions.

In addition to analytical tools, **quicR** provides flexible and customizable visualization capabilities. Leveraging the powerful ggplot2 library [21], **quicR** enables

39 users to generate high-quality, publication-ready figures. These visualizations
 40 can be further customized using the intuitive '+' syntax of ggplot2, allowing for
 41 tailored presentations of RT-QulC data.
 42 By combining standardized metrics, advanced visualization tools, and a commit-
 43 ment to open source science, **quicR** serves as a foundational tool to empower
 44 researchers to analyze and present RT-QulC data with clarity, consistency, and
 45 cohesion.

46 2. Software description

47 2.1. Software architecture

48 **quicR** was developed to address the growing need for efficient data conversion,
 49 analysis, and visualization of RT-QulC data (Figure 1). The overall architecture
 50 revolves around integration with the proprietary MARS software (BMG Labtech,
 51 Ortenberg, Germany) which exports raw data as Excel workbooks. The data
 52 from these workbooks is then curated into usable objects in the R environment,
 53 and visualized.

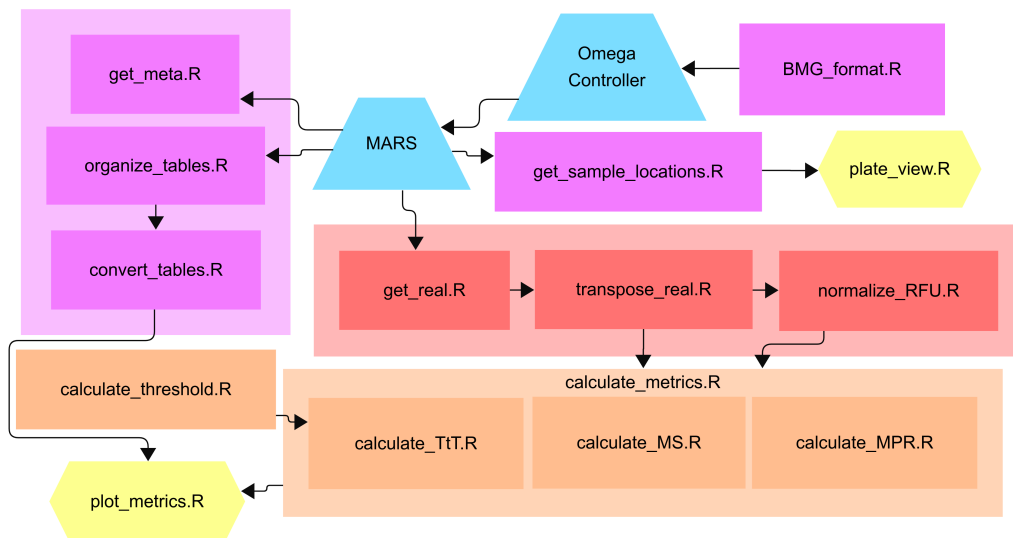


Figure 1: Workflow hierarchy of the **quicR** package. Blue nodes indicate steps where BMG software is needed. Purple nodes indicate functions dedicated to handling metadata. Red nodes are functions that acquire and manipulate raw data. Orange nodes are functions which calculate some metric. Finally, yellow nodes represent data analysis endpoints.

54 *2.2. Software functionalities*

55 The implementation of the **quicR** package encompasses several streamlined pro-
56 cesses designed to facilitate data input, cleaning, transformation, and analysis
57 of RT-QulC data. This section provides a comprehensive guide to utilizing the
58 package's key functionalities, detailing how to:

- 59 1. Format and input sample data into Omega control software (BMG Labtech,
60 Ortenberg, Germany).
- 61 2. Extract, clean, and organize metadata and raw data and apply transforma-
62 tions/normalization for downstream analysis.
- 63 3. Calculate critical analytical metrics, such as time-to-threshold (TtT), rate
64 of amyloid formation (RAF), maxpoint ratio (MPR), and maximum slope
65 (MS).
- 66 4. Visualize raw and analyzed data.

67 These steps are designed to enhance reproducibility, minimize manual data han-
68 dling, and enable seamless integration with the MARS software workflow.

69 *2.2.1. Input of Sample IDs into Omega Control Software*

70 The Omega control software allows input of a TXT file containing sample IDs,
71 dilution factors, and their well locations. This file is uniquely formatted, and not
72 easily reproduced manually.

- 73 1. **BMG_format()**: This function allows for input of a CSV file containing
74 the plate layout (see Table 1 for proper formatting), and exports the for-
75 matted TXT file. The file can then be imported into the Omega control
76 software before running.

77 *2.2.2. Data Cleaning and Transformation*

78 The MARS software exports real-time data as an Excel workbook. Typically, the
79 first sheet in the workbook will include microplate views of both raw data and
80 metadata; however, the metadata on this page is what is most useful for down-
81 stream processes. Those tables include the "Sample IDs" and "Dilutions" tables
82 (if dilutions were included in the MARS export). For much of the downstream
83 analysis, it is crucial that the "Sample IDs" table was exported from MARS. If
84 there is no table, the user can simply add it manually.

- 85 1. **organize_tables()**: returns a list of tables contained in the first sheet of
86 the exported Excel sheet. These tables contain valuable metadata such as
87 sample IDs, dilution factors, and microplate locations.
- 88 2. **convert_tables()**: accepts tables outputted from **organize_tables()** and
89 converts them to columns in a data frame.

	1	2	3	4	5	6	7	8	9	10	11	12
A	P	S01	S02	S03	S04	S05	S06	S07	S08	S09	S10	S11
B	P	S01	S02	S03	S04	S05	S06	S07	S08	S09	S10	S11
C	P	S01	S02	S03	S04	S05	S06	S07	S08	S09	S10	S11
D	P	S01	S02	S03	S04	S05	S06	S07	S08	S09	S10	S11
E	N	S01	S02	S03	S04	S05	S06	S07	S08	S09	S10	S11
F	N	S01	S02	S03	S04	S05	S06	S07	S08	S09	S10	S11
G	N	S01	S02	S03	S04	S05	S06	S07	S08	S09	S10	S11
H	N	S01	S02	S03	S04	S05	S06	S07	S08	S09	S10	S11

Table 1: Example CSV file 96-well plate layout for input into the `BMG_format()` function. The top left corner is cell "A1" in the CSV file. The top numbered row and the left-most lettered column should never be altered.

- 90 3. **get_sample_locations()**: extracts the well locations for each sample.
- 91 Output of this function is used as an argument for visualizing a microplate-
- 92 level view of real-time data.

93 2.2.3. Retrieving and Manipulating Raw Data

94 The raw, real-time data is typically found on the second sheet of the Excel work-
95 book exported from MARS. There are three functions dedicated to the retrieval
96 and cleaning of raw data.

- 97 1. **get_real()**: Retrieves the raw data from the Excel file, and outputs it as
- 98 a data frame.
- 99 2. **transpose_real()**: Swaps the rows and columns which facilitates down-
- 100 stream analyses.
- 101 3. **normalize_RFU()**: normalizes the raw data by dividing each read by
- 102 background fluorescence at a given cycle.

103 2.2.4. Calculations

104 Three analytical metrics have dedicated functions: TtT, MPR, and MS. RAF
105 does not have a designated function since it is simply the reciprocal of the time-to-
106 threshold ($1/TtT$). However, it can be calculated using the `calculate_metrics()`
107 function if TtT is chosen as an optional parameter. Each function below accepts
108 input from the `transpose_real()` or the `normalize_RFU()` functions. See Figure 2
109 for an example of the output of these functions.

- 110 1. **calculate_threshold()**: returns a value which is a given number of stan-
- 111 dard deviations above the average background fluorescence of the entire

- 112 microplate. This is a popular method of threshold calculation as reviewed
 113 in Rowden, et al.[15].
- 114 2. **calculate_TtT()**: takes the real-time data and calculates the time in
 115 hours needed to reach a given threshold value. This threshold can be
 116 supplied by `calculate_threshold()` or determined separately by the user.
 - 117 3. **calculate_MPR()**: accepts raw or normalized data and returns the max-
 118 imum value obtained during the run. If supplied with raw data, it will make
 119 a call to the `normalize_RFU()` function.
 - 120 4. **calculate_MS()**: computes the approximate derivative of the real-time
 121 data and returns the maximum value obtained during the run.
 - 122 5. **calculate_metrics()**: makes a call to functions 2–4 above and generates
 123 a data frame with the sample-matched metrics. Also computes RAF if TtT
 124 is given as an argument.

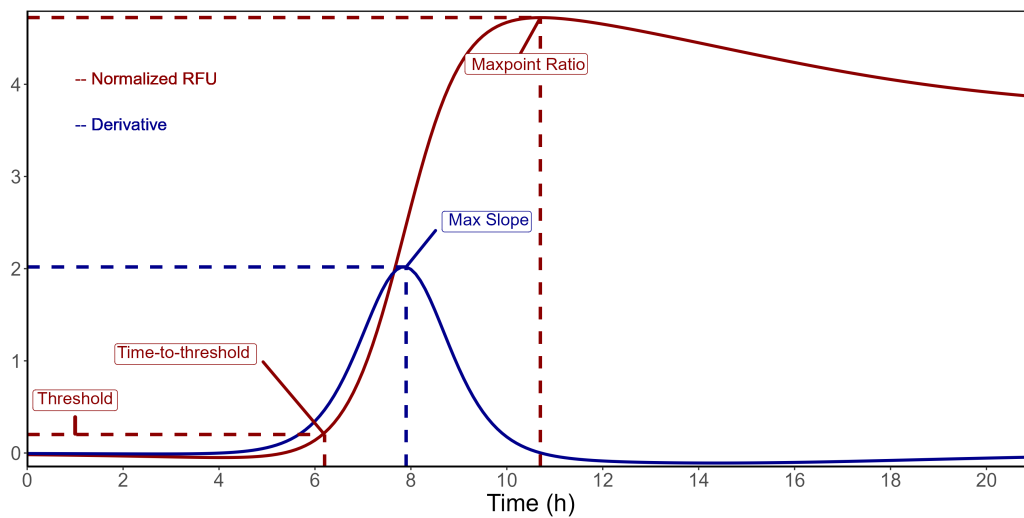


Figure 2: Example graph highlighting the calculated metrics described herein. The red curve represents a raw data curve that has been normalized against background. The maxpoint ratio is calculated as the maximum fluorescent value achieved in the normalized raw data. Time-to-threshold is determined as the time required to cross a given threshold (in this example, the threshold is set at 0.2). The blue curve represents the derivative of the raw data, and max slope is determined as the maximum of the derivative.

125 2.2.5. Visualization

126 The ensuing goal of this package is visualizing RT-QulC data. While there are
 127 many ways to represent these data, **quicR** includes two functions which provide
 128 a rapid assessment of the RT-QulC results.

- 129 1. **plate_view()**: accepts the output from the `get_real()` function and
130 `get_sample_locations()` function. Makes an 8×12 or 16×24 faceted plot
131 depending on if the plate has 96 or 384 wells. Each facet shows the real-
132 time data of each well.
- 133 2. **plot_metrics()**: requires the output of `calculate_metrics()` and gener-
134 ates a boxplot of each sample's MPR, MS, RAF, and TtT.

135 2.3. *Comparable Methods*

136 To contextualize the functionality and performance of **quicR**, we compared
137 it with existing RT-QulC analysis approaches from the published R package,
138 **QulCSeedR** [22], and the unpublished package, **rtquicR** [23]. While all three
139 offer overlapping core functionalities, their design philosophies, input handling,
140 and computational trade-offs differ substantially.

141 Benchmarking was performed using the **rbenchmark** library [24] with 50 replications
142 for each function. Comparisons are approximate, as equivalent functions were
143 not necessarily found between the three packages. Results are summarized in
144 Table 2. In general, **QulCSeedR** demonstrates the fastest execution times across
145 most core functions. However, **quicR** addresses several practical limitations
146 that the authors believe justify the slower performance in some areas. Notably,
147 **QulCSeedR** requires an additional, manually formatted Excel file to input sample
148 metadata, whereas **quicR** directly parses both raw and meta data embedded
149 within a single MARS export file. This design reduces user overhead and minimizes
150 the potential for transcription errors.

151 The **rtquicR** package introduces support for additional thresholding methods
152 and normalization strategies, and uniquely includes features such as SD50 and
153 area-under-the-curve calculations. However, it does not currently support 384-well
154 plate layouts, automated metadata parsing, or input files with missing data, all
155 of which are supported by **quicR**. Its functions also require pre-cleaned and
156 pre-structured input data, placing more burden on the user to prepare their
157 dataset prior to analysis.

158 **quicR** further distinguishes itself through its modular design, allowing users to
159 calculate metrics such as MPR, MS, TtT, and RAF independently rather than
160 as a bundled operation. While **QulCSeedR** includes built-in support for bulk
161 analysis and diagnostic outputs, these workflows can be achieved in **quicR** using
162 standard R idioms (e.g., the `apply` family of functions), and are planned for
163 future releases.

164 Overall, **quicR** favors flexibility, reproducibility, and usability with raw instrument
165 output at the expense of execution speed trade-offs that align with the package's
166 intended use in diagnostic pipelines.

Feature / Benchmark	quicR	QulCSeedR	rtquicR
Available on CRAN	Yes	Yes	No
Number of input files required	1	2	2
Number of threshold methods	2	3	4
Number of normalization methods	1	1	2
Automated metadata entry	Yes	No	No
Automated sample locations	Yes	Yes	No
Allows empty data	Yes	Yes	No
Compatible with 384-well plates	Yes	Yes	No
Built-in bulk analysis support	No	Yes	Yes
Diagnostic analysis functionality	No	Yes	No
Incorporates dilution factors	Yes	No	Yes
Converts time units	No	Yes	Yes
Calculates metrics independently	Yes	No	Yes
Calculates metrics in bulk	Yes	Yes	No
Calculates MPR	Yes	Yes	Yes
Calculates MS	Yes	Yes	No
Calculates TtT	Yes	Yes	Yes
Calculates RAF	Yes	Yes	No
Calculates area under the curve	No	No	Yes
Calculates SD50	No	No	Yes
Plate view plot execution time (s)	0.082	0.062	NA
Metric plot execution time (s)	0.009	0.005	0.007
Metric calculations (MPR, MS, etc.) (s)	0.355	0.018	NA
MPR calculation (s)	0.002	NA	0.028
TtT calculation (s)	0.001	NA	0.131
Metadata parsing time (s)	0.127	0.037	NA
Raw data parsing time (s)	0.069	0.050	0.191
Bulk analysis (s/file)	6.550	0.849	1.986

Table 2: Comparison of core features and execution times between **quicR**, QulCSeedR, and rtquicR. All benchmarks were performed using the same dataset and machine (Windows 11, 16GB RAM) in 50 replicates.

2.4. *Reproducibility*

To evaluate the reproducibility of **quicR** across systems and users, we developed a standardized script that processes MARS output files and writes three key result

170 CSV files: metadata, normalized fluorescence data, and calculated metrics as well
 171 as a plain-text file containing R session information (See Table 3). This script
 172 and accompanying raw data files were distributed, and users were instructed
 173 to source the script in the project directory. The output files were compared
 174 between each user for inconsistencies. Numerical data were given a floating
 175 point tolerance of $1E^{-12}$. Additionally, session summaries were parsed to extract
 176 R version, environment, and machine information. We did not observe any
 177 divergent results between any two users. A copy of the benchmarking script
 178 is available in the GitHub repository.

User	R Version	quicR Version	Platform	OS
1	4.4.3	2.1.0	x86_64-w64-mingw32/x64	Windows 11 x64 (build 26100)
2	4.4.1	2.1.0	aarch64-apple-darwin20	macOS 15.5
3	4.4.3	2.1.0	aarch64-apple-darwin20	macOS Sequoia 15.5
4	4.5.0	2.1.0	aarch64-apple-darwin20	macOS Sonoma 14.7.5
5	4.4.3	2.1.0	x86_64-w64-mingw32/x64	Windows 11 x64 (build 26100)
6	4.4.3	2.1.0	x86_64-w64-mingw32/x64	Windows 11 x64 (build 26100)

Table 3: User session information. The script was run on both Windows and Mac machines with a variety of R versions. The quicR versions were kept identical to ensure reproducibility.

179 2.5. Maintenance and Community Involvement

180 The **quicR** package is developed with long-term maintainability and community
 181 engagement in mind. The source code is hosted on GitHub (<https://github.com/gagerowden/quicR>)
 182 where users can report issues, request features, and contribute improvements via
 183 pull requests. A comprehensive **CONTRIBUTING** file and issue templates are
 184 provided to streamline collaboration and to facilitate external contributions. In
 185 addition to continuous integration testing, we plan to tag releases with semantic
 186 versioning and maintain a changelog to track updates and improvements. We
 187 encourage users to share their use cases, raise issues, and help shape future
 188 development directions.

189 3. Illustrative examples

190 To demonstrate the utility of **quicR**, we used a typical RT-QulC run performed
 191 on a 96-well plate. The reaction was performed on a FLUOstar Omega plate
 192 reader (BMG Labtech, Ortenberg, Germany). The file was exported as an Excel
 193 workbook where the metadata appears on the first sheet and the raw data on
 194 the second sheet.

195 3.1. Example Code

```
196 # Step 1: Install and load the package.  
197 install.packages("quicR")  
198 library(quicR)  
199 # Step 2: Identify the raw file.  
200 file <- "example.xlsx"  
201 # Step 3: Extract the raw data.  
202 raw <- get_real(file)[[1]]  
203 # Step 4: Normalize the data against the background.  
204 normal <- normalize_RFU(raw, transposed = FALSE)  
205 # Step 5: Extract the metadata.  
206 meta <- organize_tables(file) |> convert_tables()  
207 # Step 6: Get sample locations.  
208 locations <- get_sample_locations(file)  
209 # Step 7: Create the analyzed data frame.  
210 analyzed <- calculate_metrics(normal, meta)  
211 # Step 8: Plot the analyzed data frame.  
212 plot_metrics(analyzed)  
213 # Step 9: Plot the plate view.  
214 plate_view(raw, locations)
```

215
216 Once the file name is identified, ~~the~~ `get_real()` ~~function~~ is used to extract the
217 raw data. This data is imported as a data frame with each sample designated
218 as an individual column and the first column designated as time. Much of the
219 downstream analysis works best with background-normalized data, so the raw
220 data is then passed to ~~the~~ `normalize_RFU()` ~~function~~ [15]. This function accepts
221 an integer as an argument for the desired cycle to be selected for background
222 measurement.

223 Next, the metadata is extracted using ~~the~~ `organize_tables()` and `convert_tables()` ~~functions~~.
224 These take the metadata found on the first sheet of the Excel file and convert
225 them into data frame columns. Finally, metrics are calculated and assigned to
226 their given sample ID using `calculate_metrics()`. This generates a data frame
227 with sample IDs, dilution factors (if chosen), MPR's, MS's, RAF's, and TtT's.
228 Once the proper variables have been defined, they can be used as input in the
229 visualization functions. The analyzed data frame can be used as an argument in
230 `plot_metrics()` to generate a plot such as Figure 3. Additionally, the raw data
231 and sample locations are used to plot the plate view as in Figure 4.

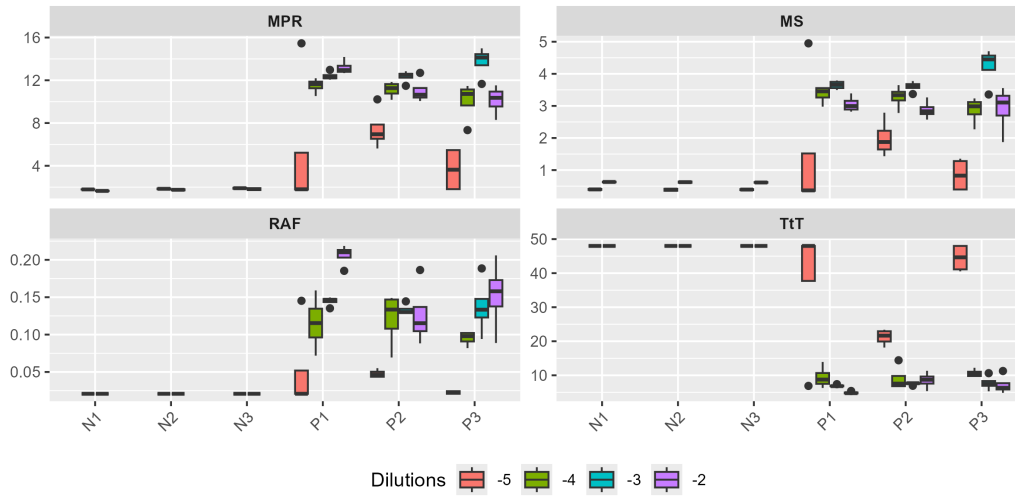


Figure 3: Boxplot of the four critical metrics calculated by the **quicR** package.

232 4. Impact

233 Since its development in 2010 [1, 2], the utility of RT-QulC has expanded to
 234 a host of neurodegenerative diseases caused by prions and other misfolded pro-
 235 teins [25, 26, 27]. The improved speed and accuracy of the assay has been a boon
 236 to human health [5, 28, 29, 30] and animal management efforts [31, 32, 33, 34].
 237 Thus, it is imperative that standardized practices and analyses are adopted.

238 The **quicR** package represents a significant advancement in the standardization
 239 and reproducibility of RT-QulC data analysis. By integrating key metrics such
 240 as TtT [5], RAF [19], MPR [15], and MS [20], **quicR** addresses critical gaps
 241 in the field, providing researchers and diagnosticians with a robust toolkit for
 242 interpreting RT-QulC data.

243 One of the primary strengths of **quicR** lies in its streamlined workflow and
 244 user-centric design. The package leverages R's powerful ecosystem and the tidy-
 245 verse [35] to create high-quality, customizable visualizations, ensuring accessi-
 246 bility for a wide range of users. Additionally, the incorporation of open-source
 247 principles allows the broader scientific community to contribute to its develop-
 248 ment, fostering innovation and adaptability.

249 Despite these strengths, there are limitations to consider. Currently, **quicR** is
 250 tailored to data exported from the MARS software, which may limit its appli-
 251 cability to researchers using alternative microplate readers. Future iterations of
 252 the package could expand compatibility by incorporating functions to handle di-
 253 verse data formats. Furthermore, while **quicR** includes robust visualization tools,
 254 users seeking highly specialized plots like those made by Li, et al. [22] may require

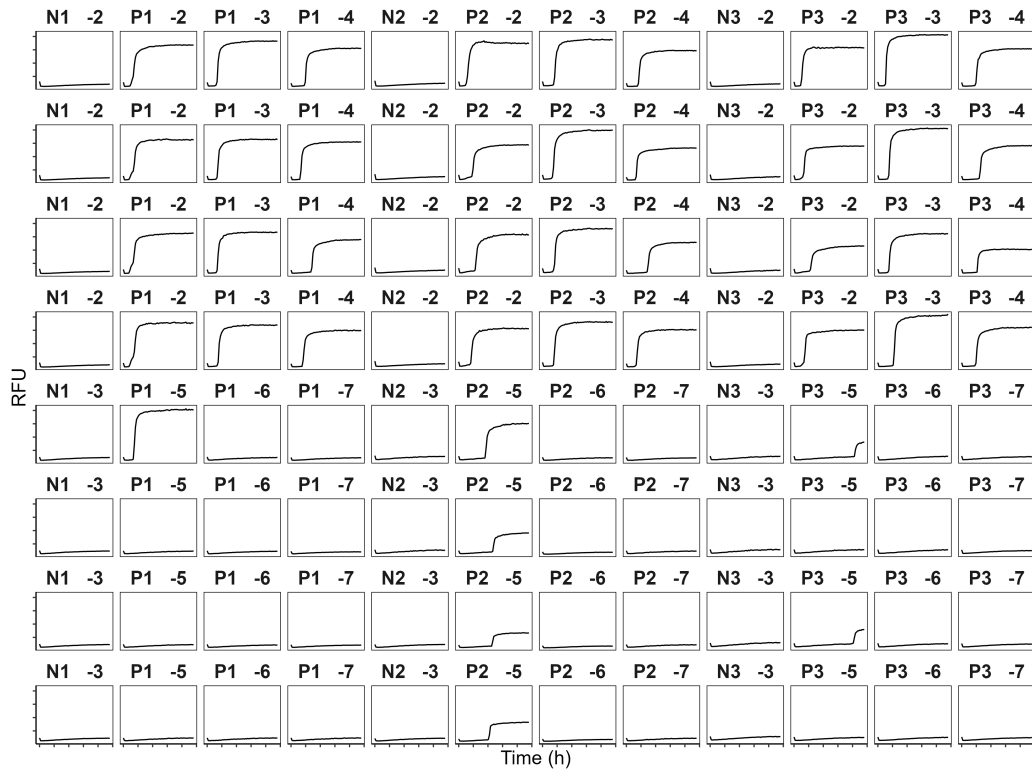


Figure 4: Plate view of RT-QulC. Wells are identified with a sample ID and dilution factor separated by an optional delimiter (in this case, a whitespace).

additional customization beyond the package's default capabilities.

Another avenue for improvement lies in the standardization of RT-QulC diagnostic criteria. **quicR** provides tools to calculate key metrics, but consensus on thresholds and diagnostic interpretations remains a challenge for the field [15]. Collaborative efforts among researchers and clinicians are necessary to define universal criteria, enabling **quicR** to fully realize its potential as a diagnostic tool. Diagnostic determinations could easily be built into the library, but a larger consensus within the research community will need to be reached to warrant inclusion.

5. Conclusions

quicR offers a powerful solution for the cleaning, analysis, and visualization of RT-QulC data, addressing critical needs in a rapidly evolving field. By enabling consistent data handling and interpretation, **quicR** provides the foundation for improved diagnostic consistency and reproducibility. The package's open-source

269 nature ensures that it will continue to evolve, integrating new insights and tech-
270 nologies as they emerge.
271 As RT-QuIC technology advances, tools like **quicR** will play a pivotal role in
272 bridging the gap between assay development and practical application. By equip-
273 ping researchers with reliable, standardized tools, **quicR** not only supports the
274 study of prion and protein misfolding disorders but also serves as a model for the
275 development of software solutions in other diagnostic fields.

276 Declaration of Conflicting Interests

277 Peter A. Larsen is a co-founder and stock owner, and Gage R. Rowden is a stock
278 owner of Priogen Corp., a diagnostic company specializing in the ultra-sensitive
279 detection of pathogenic proteins associated with prion and protein-misfolding
280 diseases. The University of Minnesota licensed patent applications to Priogen.

281 Acknowledgements

282 Special thanks to Beni Altmann at The Comprehensive R Archive Network
283 (CRAN) for help during the submission process to CRAN. We thank Tiffany
284 Wolf and Marc Schwabenlander for their support through the Minnesota Center
285 for Prion Research and Outreach. We thank Miranda Huang and Kristin Bondo
286 for testing the code. We would like to acknowledge Suzanne Stone and Sarah
287 Gresch for maintaining lab operations. We thank Sarah Gresch, Kendra Phelps,
288 Laramie Lindsey, Miranda Huang, and Kristin Bondo for their participation in the
289 reproducibility study. This work was funded by the Legislative-Citizen Commis-
290 sion on Minnesota Resources.

291 References

- 292 [1] J. M. Wilham, C. D. Orrú, R. A. Bessen, R. Atarashi, K. Sano, B. Race,
293 K. D. Meade-White, L. M. Taubner, A. Timmes, B. Caughey, Rapid end-
294 point quantitation of prion seeding activity with sensitivity comparable to
295 bioassays, PLOS Pathog 6 (12 2010). doi:10.1371/journal.ppat.
296 1001217.
- 297 [2] R. Atarashi, K. Sano, K. Satoh, N. Nishida, Real-time quaking-induced
298 conversion: A highly sensitive assay for prion detection, Prion 5 (2011)
299 150–153. doi:10.4161/pri.5.3.16893.
300 URL <https://www.ncbi.nlm.nih.gov/pmc/articles/PMC3226039/>
- 301 [3] C. D. Orrú, J. M. Wilham, L. D. Raymond, F. Kuhn, B. Schroeder, A. J.
302 Raeber, B. Caughey, Prion disease blood test using immunoprecipitation

- 303 and improved quaking-induced conversion, *mBio* 2 (3) (2012). doi:10.
304 1128/mBio.00078-11.
- 305 [4] C. D. Orrù, B. R. Groveman, A. G. Hughson, M. Manca, L. D. Raymond,
306 G. J. Raymond, K. J. Campbell, K. J. Anson, A. Kraus, B. Caughey, RT-
307 QulC assays for prion disease detection and diagnostics, in: *Methods in*
308 *Molecular Biology*, Vol. 1658, Humana Press Inc., 2017, pp. 185–203.
- 309 [5] C. D. Orrù, B. R. Groveman, A. G. Hughson, G. Zanusso, M. B.
310 Coulthart, B. Caughey, Rapid and sensitive rt-quic detection of human
311 creutzfeldt-jakob disease using cerebrospinal fluid, *mBio* 6 (1 2015).
312 doi:10.1128/mBio.02451-14.
313 URL /pmc/articles/PMC4313917//pmc/articles/PMC4313917/
314 ?report=abstracthttps://www.ncbi.nlm.nih.gov/pmc/articles/
315 PMC4313917/
- 316 [6] M. Bongianni, A. Ladogana, S. Capaldi, S. Klotz, S. Baiardi, A. Cagnin,
317 D. Perra, M. Fiorini, A. Poleggi, G. Legname, T. Cattaruzza, F. Janes,
318 M. Tabaton, B. Ghetti, S. Monaco, G. G. Kovacs, P. Parchi, M. Pocchiari,
319 G. Zanusso, α -Synuclein RT-QulC assay in cerebrospinal fluid of patients
320 with dementia with lewy bodies, *Annals of Clinical and Translational Neu-*
321 *rology* 6 (10) (2019) 2120–2126.
- 322 [7] R. P. Dassanayake, C. D. Orrù, A. G. Hughson, B. Caughey, T. Graça,
323 D. Zhuang, S. A. Madsen-Bouterse, D. P. Knowles, D. A. Schneider, Sensi-
324 tive and specific detection of classical scrapie prions in the brains of goats by
325 real-time quaking-induced conversion, *J. Gen. Virol.* 97 (3) (2016) 803–812.
- 326 [8] S. Hwang, M. H. West Greenlee, A. Balkema-Buschmann, M. H. Groschup,
327 E. M. Nicholson, J. J. Greenlee, Real-time quaking-induced conversion de-
328 tection of bovine spongiform encephalopathy prions in a subclinical steer,
329 *Frontiers in Veterinary Science* 4 (JAN) (2018) 19.
- 330 [9] B. R. Groveman, C. D. Orrù, A. G. Hughson, L. D. Raymond, G. Zanusso,
331 B. Ghetti, K. J. Campbell, J. Safar, D. Galasko, B. Caughey, Rapid and
332 ultra-sensitive quantitation of disease-associated α -synuclein seeds in brain
333 and cerebrospinal fluid by α Syn RT-QulC, *Acta Neuropathologica Commu-*
334 *nications* 6 (1) (2018) 7.
- 335 [10] M. A. Metrick, 2nd, N. d. C. Ferreira, E. Saijo, A. Kraus, K. Newell,
336 G. Zanusso, M. Vendruscolo, B. Ghetti, B. Caughey, A single ultrasensi-
337 tive assay for detection and discrimination of tau aggregates of alzheimer
338 and pick diseases, *Acta Neuropathol Commun* 8 (1) (2020) 22.

- [11] M. Fiorini, G. Iselle, D. Perra, M. Bongiani, S. Capaldi, L. Sacchetto, S. Ferrari, A. Mombello, S. Vascellari, S. Testi, S. Monaco, G. Zanusso, High diagnostic accuracy of rt-quic assay in a prospective study of patients with suspected scjd, *International Journal of Molecular Sciences* 21 (3) (2020). doi:10.3390/ijms21030880. URL <https://www.mdpi.com/1422-0067/21/3/880>
- [12] A. Franceschini, S. Baiardi, A. G. Hughson, N. McKenzie, F. Moda, M. Rossi, S. Capellari, A. Green, G. Giaccone, B. Caughey, P. Parchi, High diagnostic value of second generation csf rt-quic across the wide spectrum of cjd prions, *Sci Rep* (9 2017). doi:10.1038/s41598-017-10922-w.
- [13] C. Picasso-Risso, M. D. Schwabenlander, G. Rowden, M. Carstensen, J. C. Bartz, P. A. Larsen, T. M. Wolf, Assessment of Real-Time Quaking-Induced conversion (RT-QulC) assay, immunohistochemistry and ELISA for detection of chronic wasting disease under field conditions in White-Tailed deer: A bayesian approach, *Pathogens* 11 (5) (2022).
- [14] C. L. Holz, J. R. Darish, K. Straka, N. Grosjean, S. Bolin, M. Kiupel, S. Sreevatsan, Evaluation of Real-Time Quaking-Induced conversion, ELISA, and immunohistochemistry for chronic wasting disease diagnosis, *Front Vet Sci* 8 (2021) 824815.
- [15] G. R. Rowden, C. Picasso-Risso, M. Li, M. D. Schwabenlander, T. M. Wolf, P. A. Larsen, Standardization of data analysis for rt-quic-based detection of chronic wasting disease, *Pathogens* 12 (2023) 309. doi:10.3390/PATHOGENS12020309/S1. URL <https://www.mdpi.com/2076-0817/12/2/309/html><https://www.mdpi.com/2076-0817/12/2/309>
- [16] R Core Team, R: A Language and Environment for Statistical Computing, R Foundation for Statistical Computing, Vienna, Austria (2024). URL <https://www.R-project.org/>
- [17] P. R. Christenson, M. Li, G. Rowden, P. A. Larsen, S.-H. Oh, Nanoparticle-enhanced rt-quic (nano-quic) diagnostic assay for misfolded proteins, *Nano Letters* 23 (9) (2023) 4074–4081, pMID: 37126029. arXiv:<https://doi.org/10.1021/acs.nanolett.3c01001>, doi:10.1021/acs.nanolett.3c01001. URL <https://doi.org/10.1021/acs.nanolett.3c01001>
- [18] D. J. Lee, P. R. Christenson, G. Rowden, N. C. Lindquist, P. A. Larsen, S.-H. Oh, Rapid on-site amplification and visual detection of misfolded

- 375 proteins via microfluidic quaking-induced conversion (micro-quic), npj
376 Biosensing 1 (6) (7 2024). doi:10.1038/s44328-024-00006-x.
377 URL [https://www.nature.com/articles/s44328-024-00006-x#](https://www.nature.com/articles/s44328-024-00006-x#citeas)
378 citeas
- 379 [19] N. J. Gallups, A. S. Harms, ‘seeding’ the idea of early diagnostics in synu-
380 cleinopathies, Brain 145 (2022) 418–419. doi:10.1093/BRAIN/AWAC062.
381 URL <https://dx.doi.org/10.1093/brain/awac062>
- 382 [20] D. M. Henderson, K. A. Davenport, N. J. Haley, N. D. Denkers, C. K.
383 Mathiason, E. A. Hoover, Quantitative assessment of prion infectivity in
384 tissues and body fluids by real-time quaking-induced conversion, Journal of
385 General Virology 96 (2015) 210–219. doi:10.1099/vir.0.069906-0.
- 386 [21] H. Wickham, ggplot2: Elegant Graphics for Data Analysis, Springer-Verlag
387 New York, 2016.
388 URL <https://ggplot2.tidyverse.org>
- 389 [22] M. Li, D. N. Bryant, S. Gresch, M. S. Milstein, P. R. Christenson, S. S.
390 Lichtenberg, P. A. Larsen, S. H. Oh, QulCSeedR: An R package for analyzing
391 fluorophore-assisted seed amplification assay data, Bioinformatics 41 (1)
392 (2025) 1–7. doi:10.1093/bioinformatics/btae752.
- 393 [23] J. Slota, rtquicr, <https://github.com/jslota/rtquicR> (2023).
- 394 [24] W. Kusnierczyk, rbenchmark: Benchmarking routine for R, r package ver-
395 sion 1.0.0 (2012).
396 URL <https://CRAN.R-project.org/package=rbenchmark>
- 397 [25] C. D. Orrú, B. R. Groveman, A. G. Hughson, T. Barrio, K. Isiofia, B. Race,
398 N. C. Ferreira, P. Gambetti, D. A. Schneider, K. Masujin, K. Miyazawa,
399 B. Ghetti, G. Zanusso, B. Caughey, Sensitive detection of pathological seeds
400 of α -synuclein, tau and prion protein on solid surfaces, PLOS Pathogens
401 20 (4) (2024) 1–22. doi:10.1371/journal.ppat.1012175.
402 URL <https://doi.org/10.1371/journal.ppat.1012175>
- 403 [26] E. Alwakil, Chapter 6 - α -synuclein seeding assay and analysis, in:
404 W. Mohamed (Ed.), Translational Models of Parkinson’ s Disease
405 and Related Movement Disorders, Academic Press, 2025, pp. 97–109.
406 doi:<https://doi.org/10.1016/B978-0-443-16128-5.00006-2>.
407 URL [https://www.sciencedirect.com/science/article/pii/](https://www.sciencedirect.com/science/article/pii/B9780443161285000062)
408 B9780443161285000062

- [27] Z. Wang, L. Wu, M. Gerasimenko, T. Gilliland, S. A. Gunzler, V. Donadio, R. Liguori, B. Xu, W.-Q. Zou, R. Article, Seeding Activity of Skin Misfolded Tau as a Biomarker for Tauopathies, *Molecular Neurodegeneration* (2024) 1–19doi:10.1186/s13024-024-00781-1.
URL <https://doi.org/10.21203/rs.3.rs-3968879/v1>
- [28] A. J. Green, Rt-quic: a new test for sporadic cjd, *Practical neurology* 19 (1) (2019) 49–55.
- [29] B. Race, K. Williams, B. Chesebro, Transmission studies of chronic wasting disease to transgenic mice overexpressing human prion protein using the rt-quic assay, *Veterinary research* 50 (1) (2019) 6.
- [30] S. Vascellari, C. D. Orrù, B. Caughey, Real-time quaking-induced conversion assays for prion diseases, synucleinopathies, and tauopathies, *Frontiers in Aging Neuroscience* 14 (2022) 853050.
- [31] M. H. Huang, S. Demarais, M. D. Schwabenlander, B. K. Strickland, K. C. VerCauteren, W. T. McKinley, G. Rowden, C. C. Valencia Tibbitts, S. C. Gresch, S. S. Lichtenberg, et al., Chronic wasting disease prions on deer feeders and wildlife visitation to deer feeding areas, *The Journal of Wildlife Management* (2025) e70000.
- [32] S. K. Cooper, C. E. Hoover, D. M. Henderson, N. J. Haley, C. K. Mathiason, E. A. Hoover, Detection of cwd in cervids by rt-quic assay of third eyelids, *PloS one* 14 (8) (2019) e0221654.
- [33] R. B. Piel III, S. E. Veneziano, E. M. Nicholson, D. P. Walsh, A. D. Lomax, T. A. Nichols, C. M. Seabury, D. A. Schneider, Validation of a real-time quaking-induced conversion (rt-quic) assay protocol to detect chronic wasting disease using rectal mucosa of naturally infected, pre-clinical white-tailed deer (*odocoileus virginianus*), *PLoS One* 19 (6) (2024) e0303037.
- [34] E. Harpaz, F. A. Cazzaniga, L. Tran, T. T. Vuong, G. Bufano, Ø. Salvesen, M. Gravdal, D. Aldaz, J. Sun, S. Kim, et al., Transmission of norwegian reindeer cwd to sheep by intracerebral inoculation results in an unusual phenotype and prion distribution, *Veterinary Research* 55 (1) (2024) 94.
- [35] H. Wickham, M. Averick, J. Bryan, W. Chang, L. D. McGowan, R. François, G. Golemund, A. Hayes, L. Henry, J. Hester, M. Kuhn, T. L. Pedersen, E. Miller, S. M. Bache, K. Müller, J. Ooms, D. Robinson, D. P. Seidel, V. Spinu, K. Takahashi, D. Vaughan, C. Wilke, K. Woo, H. Yutani, Welcome to the tidyverse, *Journal of Open Source Software* 4 (43) (2019) 1686. doi:10.21105/joss.01686.